European Journal of Radiology 113 (2019) 51–58

Contents lists available at ScienceDirect

European Journal of Radiology

journal homepage: www.elsevier.com/locate/ejrad

Research article

A comparison of the reproducibility of two cine-derived strain software programmes in disease states

M.P. Graham-Brown[a,b,c], G.S. Gulsin[d], K. Parke[d], J. Wormleighton[d], F.Y. Lai[d], L. Athithan[d], J.R. Arnold[d], J.O. Burton[a,b], G.P. McCann[d,*], A.S. Singh[d]

[a] John Walls Renal Unit, University Hospitals Leicester NHS Trust, UK
[b] Department of Infection Immunity and Inflammation, School of Medicine and Biological Sciences, University of Leicester, UK
[c] National Centre of Sport and Exercise Medicine, University of Loughborough, UK
[d] Dept of Cardiovascular Sciences, University of Leicester and NIHR Leicester Cardiovascular Biomedical Research Centre, Glenfield Hospital Leicester, UK

ARTICLE INFO

Keywords:
Strain
Reproducibility
Dialysis
Aortic stenosis
Diabetes

ABSTRACT

Background: Systolic strain and peak-early diastolic strain rate (PEDSR) measure subclinical cardiac dysfunction. These parameters can be derived from cardiovascular magnetic resonance (CMR) cine images using new software packages, but the comparative test-retest reproducibility of these software in disease states is unknown. This study compared the test-retest reproducibility of strain measures derived from two software packages (feature-tracking software (FT) and tissue-tracking (TT)) in disease populations with preserved ejection fractions.

Methods: This was a prospective study of 10 patients with aortic stenosis (AS), 10 haemodialysis patients and 10 diabetic patients at 1.5 and 3-Tesla. 30 subjects underwent test-retest reproducibility scans of global circumferential strain (GCS), global longitudinal strain (GLS), circumferential-PEDSR and longitudinal-PEDSR calculated using TT and FT software.

Results: Test-retest reproducibility of GCS and GLS were similar for FT and TT across patient groups. Coefficient of variability (CoV) for FT-derived GCS 8.1%, 5% and 7.9% for AS, diabetic and haemodialysis patients, compared to 3.3%, 9.2% and 5.4% for TT-derived GCS, with CoV for FT-derived GLS 8%, 6.4% and 8.2% for AS, diabetic and haemodialysis patients, compared to 5.3%, 4.8% and 7% for TT-derived GLS). Reproducibility of FT-derived circumferential and longitudinal-PEDSR was worse than TT-derived circumferential and longitudinal-PEDSR (CoV for FT-derived circumferential-PEDSR 18.2%, 18% and 17.4% for AS, diabetic and haemodialysis patients, compared to 6.1%, 11.7% and 11% for TT-derived circumferential-PEDSR with CoV for FT-derived longitudinal PEDSR 18.2%, 18.9%, 18.3% for AS, diabetic and haemodialysis patients, compared to 8.9%, 9.1% and 11.4% for TT-derived longitudinal-PEDSR). Bland-Altman analysis revealed no systematic bias with tighter limits of agreement for TT-derived strain measures.

Conclusions: Reproducibility of GCS and GLS are excellent with FT and TT software across diseases. TT had superior test-retest reproducibility for quantification of longitudinal and circumferential-PEDSR than FT-derived PEDSR across diseases.

1. Introduction

Left ventricular (LV) systolic strain and early diastolic strain rates are increasingly recognised measures of subclinical cardiac dysfunction. Although LV ejection fraction (EF) remains crucial to aid clinical decision-making and provide prognostic information, multiple studies have shown the additional incremental benefit of myocardial strain assessment in providing prognostic and earlier diagnostic information in disease states [1–5]. Left ventricular strain assessment with cardiac magnetic resonance imaging (CMR) has traditionally been done with myocardial tissue tagging. Strain derived from tissue tagging requires the acquisition of additional images, lengthening scan times, with semi-automated, time consuming post-processing and analysis [6]. Tagging cannot be carried out retrospectively on existing CMR datasets and myocardial tagging may suffer from progressive attenuation of the tag signal during the cardiac cycle [7]. These limitations have hindered the widespread uptake of tissues tagging in both clinical and research settings [8].

* Corresponding author at: Department of Cardiovascular Sciences, University of Leicester, Leicester, LE1 9HN, UK.
E-mail address: gpm12@le.ac.uk (G.P. McCann).

https://doi.org/10.1016/j.ejrad.2019.01.026
Received 10 September 2018; Received in revised form 11 December 2018; Accepted 22 January 2019

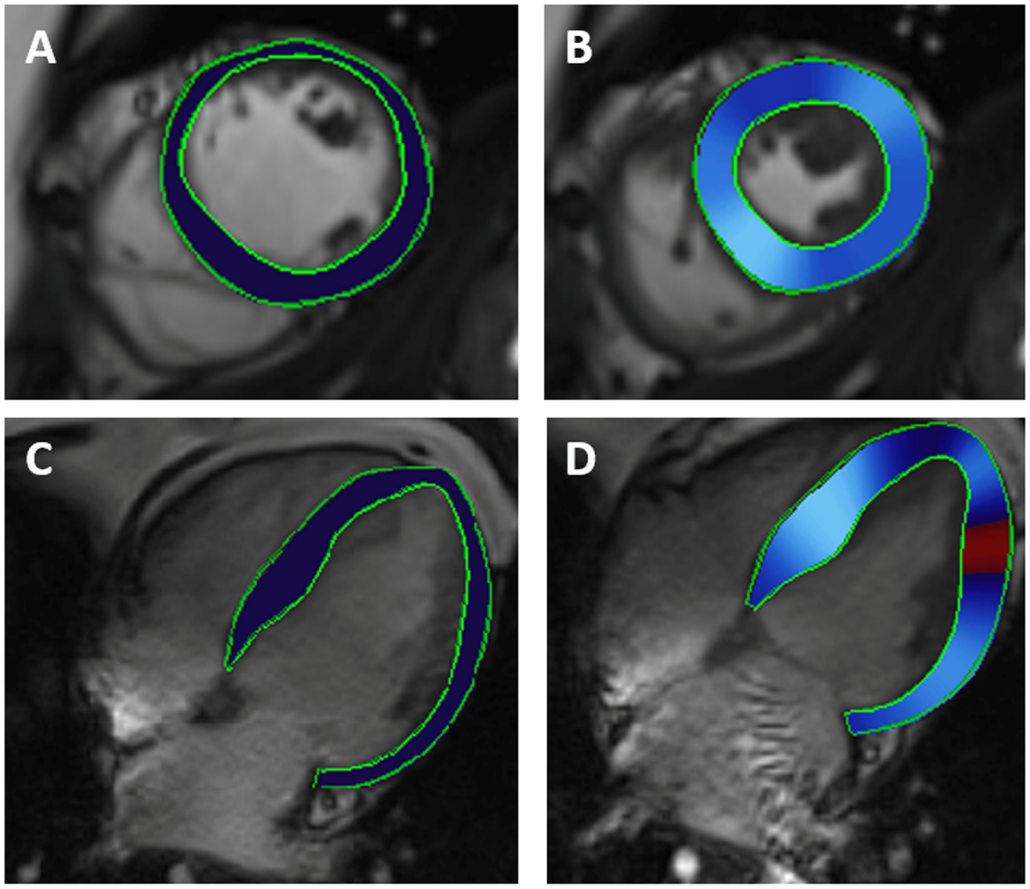

Fig. 1. Typical imaging tracking using Feature Tracking software for A: Mid-ventricular short-axis slice in end-diastole to B end-systole. C 4-chamber long-axis in end-diastole to D: end-systole.

A variety of software packages now allow quantification of myocardial strain indices directly from steady state free procession (SSFP) cine sequences. Such programs automatically track image features at the cavity-tissue interface throughout the cardiac cycle in a similar way to speckle tracking on echocardiography [9], indeed reasonable agreement has been shown between speckle-tracking derived stain and strain derived from cine images using CMR [10]. A recent study showed that whilst strain values derived from cine images using different software packages had reasonable agreement with strain values derived from tagged images, the inter-software agreement was not good [11]. The comparable test-retest reproducibility of cine-derived strain techniques are not known in disease states and given the increasing prognostic significance of strain assessment, understanding the comparable reproducibility of cine-derived strain measures using different software packages is essential for assessing disease progression or response to treatment.

The aim of this study was to compare the test-retest reproducibility of LV strain measures derived from two commercially available software packages in a range of disease states in subjects with preserved ejection fraction.

2. Material and methods

All patients were recruited prospectively at a single regional cardiac imaging center as part of three larger studies: PRIMID-AS, CYCLE-HD and DIASTOLIC [12,13]. All studies received local research and ethics approval with written informed consent from all study participants. Cardiac MRI scans for PRIMID-AS and CYCLE-HD were conducted at 3-Tesla (Skyra), whilst CMR scans for DIASTOLIC were conducted at 1.5-Tesla (Aera, both Siemens Medical Imaging, Erlangen, Germany) to standard protocols as previously described [14]. PRIMID-AS, CYCLE-HD and DIASTOLIC all included pre-specified CMR reproducibility sub-studies, where 10 patients in each study gave additional consent to return for repeat CMR scan within 14 days of initial scan [12,13]. As planned, 30 patients completed test-retest reproducibility scans; 10 asymptomatic patients with moderate-severe AS, 10 patients on maintenance haemodialysis and 10 asymptomatic patients with type 2 diabetes. This study is a post-hoc analysis of the reproducibility of cine-derived strain in disease states using two currently available software packages. Haemodialysis patients were scanned on their non-dialysis day, not after their long-break to standardize their volume status as far as possible.

2.1. CMR image acquisition

Steady state free precession end-expiratory breath-held cine images were acquired, with retrospective electrocardiogram triggering, to determine LV volumes, mass and function as previously described using an 18-channel coil at 3-Tesla and a 6-channal coil at 1.5-Tesla [15,16]. Short-axis cine images covering the entire left ventricle were taken with typical parameters at both field strengths as previously reported [16].

2.2. Image analysis

All analysis was performed off-line, blinded to patient and scan details. LV mass and volumetric analysis was conducted as previously described using CMR-42 [17,18]. Image quality of LV short and long axis cines was categorized as ‘excellent’: no artifact in any images; ‘good’: artifact present but not affecting LV; ‘moderate’: artifact present in LV but analysis still possible; and ‘unanalyzable’: artifact renders

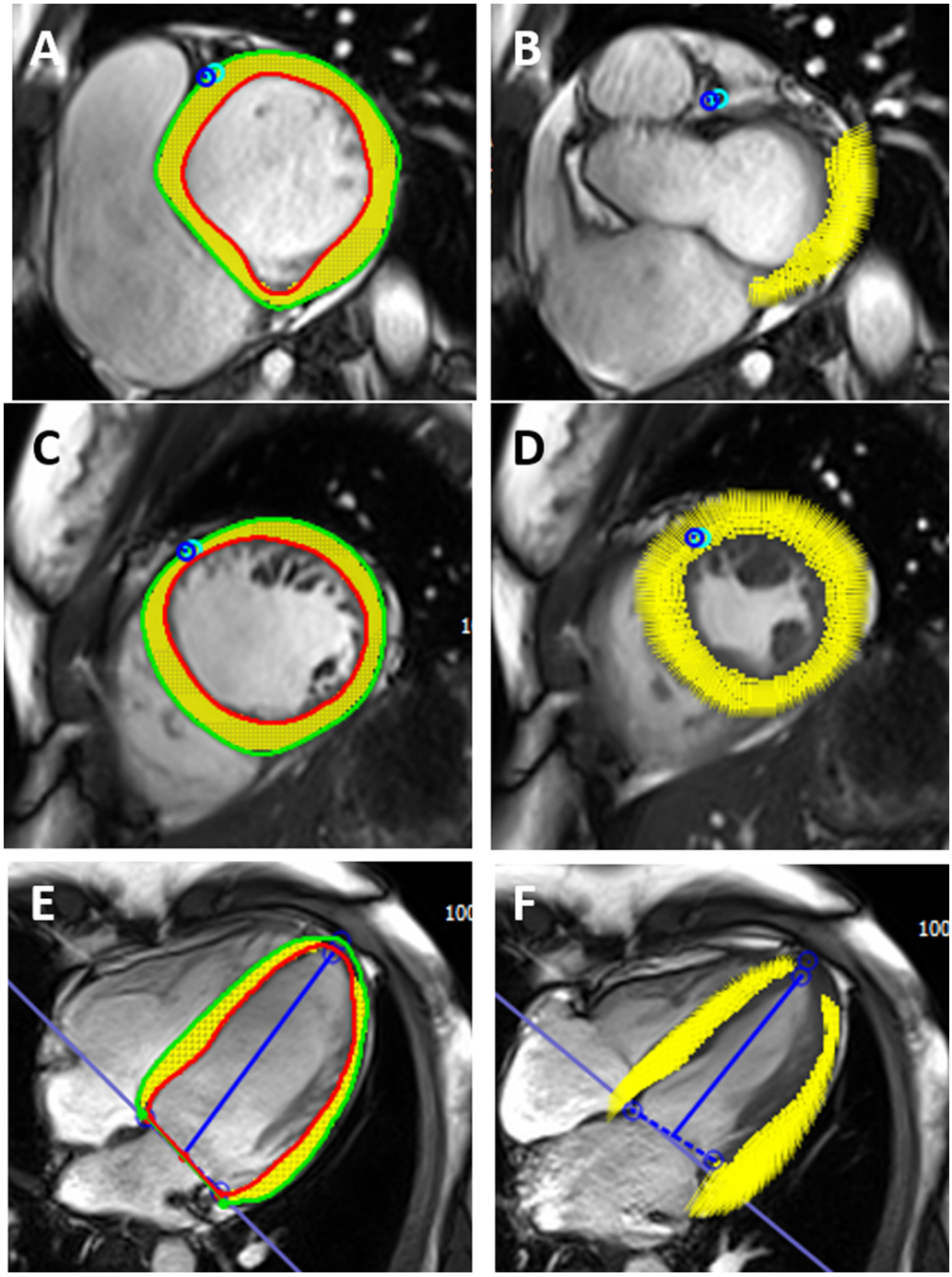

Fig. 2. Typical imaging tracking using Tissue Tracking software for A: Basal ventricular short-axis slice in end-diastole to B: end-systole. Based on the LV extent on long-axis cine images, the software automatically excludes short-axis basal slices which no longer contain myocardium as the ventricle shortens through systole. C: Mid-ventricular short axis slice in end-diastole to D: end-systole. E: 4-chamber long-axis image in end-diastole with definition of LV-extent (blue 'T') to F: end-systole. Note LV-extent tracked in all long axis cines and is used to define the extent of the left ventricle at all points in the cardiac cycle for short axis strain analysis.

scan uninterpretable. Global circumferential strain (GCS), global longitudinal strain (GLS), peak early diastolic circumferential strain rate (cPEDSR) and peak early diastolic longitudinal strain rate (lPEDSR) were calculated using TT, FT software as described below. Time taking to load scans and complete strain analysis with both software packages was recorded.

2.3. Tissue tracking strain analysis (Circle CVI, CMR-42 software)

Short and long axis cine images were loaded into the CMR-42 TT prototype module. These included the original endocardial and epicardial end-diastolic contours defined for prior volumetric and function quantification. The superior and inferior right ventricular insertion points were additionally defined on short axis cines, as well as the LV extent on long-axis cines (Fig. 1). The software automatically tracked features throughout the cardiac cycle to define strain parameters. Based on the LV extent defined from the long-axis cines, the software automatically excluded SA basal and apical slices no longer containing myocardium as the ventricle shortens and lengthens through the cardiac cycle. All TT strain analysis was carried out by a single, blinded observer. Interobserver variability of TT was assessed in 10 scans by two blinded observers.

Table 1
Baseline demographic and left ventricular mass and volume data.

	Haemodialysis patients (n = 10)	Aortic stenosis patients (n = 10)	Diabetic patients (n = 10)	All patients (n = 30)
Age (years)	57.8 ± 15	67.3 ± 9.8	48.8 ± 7.5	58 ± 13.3
Sex (% male)	8 (80%)	8 (80%)	5 (50%)	21 (70%)
BMI (kg/m^2)	25.7 ± 2.1	25.6 ± 3.4	36.2 ± 3.7	29.2 ± 5.9
SBP (mmHg)	143 ± 33	156.8 ± 23.1	147 ± 20	145.4 ± 28
DBP (mmHg)	80 ± 15	78.6 ± 12.1	88.9 ± 7.3	80.8 ± 17.1
Heart rate (beats per minute)	72.8 ± 11.2	72.1 ± 8.5	71.6 ± 11.5	72 ± 11
Medical and drug history				
Hypertension (n, %)	8 (80%)	4 (40%)	6 (60%)	18 (60%)
Diabetes (n, %)	3 (30%)	1 (10%)	10 (100%)	14 (46.7%)
CAD (n, %)	3 (30%)	2 (20%)	0 (0%)	5 (16.7%)
Previous MI (n, %)	1 (10%)	1 (10%)	0 (0%)	2 (6.7%)
PVD (n, %)	0 (0%)	0 (0%)	0 (0%)	0 (0%)
ACEi (n, %)	3 (30%)	0 (0%)	3 (30%)	6 (20%)
ARB (n, %)	1 (10%)	1 (10%)	3 (30%)	5 (16.7%)
Diuretic (n, %)	1 (10%)	1 (10%)	2 (20%)	4 (13.3%)
Beta-Blocker (n, %)	4 (40%)	4 (40%)	0 (0%)	8 (26.7%)
Statin (n, %)	4 (40%)	7 (70%)	6 (60%)	17 (56.7%)
CCB (n, %)	3 (30%)	3 (30%)	2 (20%)	8 (26.7%)
No. of anti-hypertensives (n,%)	0.96 ± 0.9	0.9 ± 0.74		
Left ventricle structural and functional data				
LVEF (%)	54.3 ± 7.7	58.6 ± 4.7	61.3 ± 5.9	58.1 ± 6.5
LV Mass (g)	95.2 ± 22	105.5 ± 20.1	111.7 ± 24.2	104.1 ± 22.5
LVMi (g/m^2)	55.8 ± 13	56.8 ± 6.5	57.8 ± 13.5	56.1 ± 11.1
LVEDV (ml)	139.3 ± 21	148.8 ± 28	164.2 ± 33.1	150.8 ± 28.8
LVM/LVEDV (g/ml)	0.68 ± 0.13	0.72 ± 0.16	0.69 ± 0.10	0.7 ± 0.12

SBP, systolic blood pressure; DBP, diastolic blood pressure; CAD, coronary artery disease; MI, myocardial infarction; PVD, peripheral vascular disease; ACEi, angiotensin converting enzyme inhibitor; ARB, angiotensin-receptor blocker; CCB, calcium channel blocker; LVEF, left ventricular ejection fraction; LVM, left ventricular mass; LVEDV, left ventricular end-diastolic volume.

2.4. Feature tracking (diogenes, tomtec software)

Short and long-axis cine images were loaded into the Diogenes FT software package. Endo and epicardial contours were drawn on a single end-diastolic phase and propagated automatically by the software to all phases, generating endocardial strain and strain rate curves (Fig. 2). If the contours did not track the borders well, the contour on the original phase was manually adjusted and re-propagated. No further post-processing was required, as the software generated both strain and strain rate graphs. Details of the algorithm used by this software have been described previously [19]. All FT strain analysis was carried out by a single, blinded observer. Interobserver variability of FT was assessed in 10 scans by two blinded observers.

2.5. Statistical analysis

Statistical analysis were undertaken using SPSS-22 software (Statistical Package for the Social Sciences, Chicago, IL, USA) and Graphpad Prism version 6.04 (GraphPad Software, Inc., La Jolla, CA, USA). Normality was assessed using the Shapiro–Wilk test, histograms, and Q−Q plots. Normally distributed data are expressed as mean ± standard deviation and non-normally distributed data are expressed as median (interquartile range). Test-retest reproducibility for subjects undergoing test-retest scans were compared using paired t-tests, co-efficients of variation (CoV) and the Bland-Altman method [20]. For each subject and technique, the squared difference between test-retest results was used as an estimate of the within-subject variance for the method. This was then log-transformed and a paired *t*-test method was used to compare test 1- with test 2-squared differences, as previously described [21,22]. The sample sizes required for all strain measures derived from TT and FT to detect a 10% between group treatment effect (enrollment ratio 1:1) were calculated based on the means and standard deviation of all test-rests scans for each patient group with powers of 80% and 90% and an α error of 0.05 [23].

Interobserver variability of TT and FT was assessed using paired t-tests, co-efficients of variation and the Bland-Altman method.

3. Results

Baseline demographic details of patient groups and LV dimensions are shown in Table 1. Median time between inter-study scans was 7 days [4,11]. All 60 scans were analyzable, with image quality assessed as excellent n = 10 (diabetic patients n = 4, aortic stenosis patients n = 3, haemodialysis patients n = 3), good n = 42 (diabetic patients n = 16, aortic stenosis patients n = 14, haemodialysis patients n = 12), moderate n = 8 (aortic stenosis patients n = 3, haemodialysis patients n = 5). Mean time taken to load images and analyse all strain measures for a single scan for FT software was 29 min compared to 6 min using TT software. No manual adjustment of contours with the TT software package was required. Minor adjustment of 8 contours was required with the FT software packages.

4. Comparison of TT and FT absolute strain values

All strain measures derived from FT software were consistently significantly higher than strain measures derived from TT software (figure S1).

5. Test-retest reproducibility of TT and FT derived strain values

The test-retest reproducibility of TT and FT derived strain values for the three patient groups are shown in Table 2. Reproducibility of GCS and GLS was similar for all patient groups and differences between reproducibility were not significantly different (all $p > 0.05$). The reproducibility of FT-derived circumferential PEDSR was significantly worse than TT derived circumferential PEDSR for patients with aortic stenosis, diabetes and patients on haemodialysis ($p < 0.01$, $p = 0.02$ and $p = 0.02$ respectively). For patients with diabetes, the

Table 2
Inter-study reproducibility of strain measures assessed by feature tracking and tissue tracking.

	Scan 1	Scan 2	CoV (%)	Bias ± SD Difference	BA limits of agreement
Feature Tracking derived stain parameters					
Aortic stenosis patients (3-Tesla) (n = 10)					
GCS	−34.1 ± 5	−29.9 ± 4.5	8.1	−4.2 ± 3.1	−10.3, 1.9
GLS	−18.2 ± 3.4	−18.7 ± 3.2	8	0.42 ± 3.1	−5.6, 6.4
cPEDSR	1.94 ± 0.4	1.6 ± 0.5	18.2	−0.33 ± 0.6	−1.5, 0.8
lPEDSR	0.88 ± 0.3	0.86 ± 0.3	18.2	−0.03 ± 0.3	−0.7, 0.6
Diabetic patients (1.5-Tesla) (n = 10)					
GCS	−38.1 ± 5.6	36.4 ± 6	5	−1.7 ± 3.5	−8.6, 5.2
GLS	−22.5 ± 3.2	−23.4 ± 3.9	6.4	0.85 ± 2.9	−4.9, 6.6
cPEDSR	0.84 ± 0.14	1 ± 0.1	18	−0.23 ± 0.7	−1.6, 1.1
lPEDSR	0.8 ± 0.2	0.8 ± 0.08	18.9	0.25 ± 0.4	−0.5, 1
Haemodialysis patients (3-Tesla) (n = 10)					
GCS	−30.1 ± 5	−32.9 ± 6.2	7.9	2.9 ± 4.5	−6, 11.7
GLS	−19.8 ± 3.7	−18.7 ± 2.5	8.2	−1.1 ± 3	−6.9, 4.7
cPEDSR	1.7 ± 0.4	1.8 ± 0.8	17.4	0.12 ± 0.6	−1.1, 1.4
lPEDSR	1.1 ± 0.3	1 ± 0.3	18.3	0.04 ± 0.4	−0.9, 0.7
All participants (both field strengths) (n = 30)					
GCS	−34.1 ± 6	−33.1 ± 6.1	7.2	−1 ± 4.7	−10.2, 8.2
GLS	−20.2 ± 3.8	−20.2 ± 3.9	7.3	0.06 ± 3	−5.9, 6
cPEDSR	1.9 ± 0.5	1.7 ± 0.7	17.4	−0.15 ± 0.6	−1.4, 1.1
lPEDSR	1 ± 0.3	0.9 ± 0.5	28.4	−0.06 ± 0.6	−1.2, 1
Tissue Tracking derived stain parameters					
Aortic stenosis patients (3-Tesla) (n = 10)					
GCS	−19.3 ± 2.7	−18.9 ± 1.7	3.3	−0.36 ± 1.6	−3.4, 2.7
GLS	−15.3 ± 2.6	−15.7 ± 1.8	5.3	0.38 ± 2.6	−4.6, 5.4
cPEDSR	0.92 ± 0.13	0.9 ± 0.16	6.1	0.02 ± 0.09	−0.2, 0.2
lPEDSR	0.75 ± 0.17	0.84 ± 0.16	8.9	−0.09 ± 0.2	−0.5, 0.3
Diabetic patients (1.5-Tesla) (n = 10)					
GCS	−20.3 ± 2.5	−17.2 ± 3.4	9.2	3.1 ± 1.6	−0.07, 6.3
GLS	−16.2 ± 2.1	−16.3 ± 3.2	4.8	−0.03 ± 1.7	−3.3, 3.2
cPEDSR	0.84 ± 0.14	1 ± 0.1	11.7	−0.2 ± 0.1	−0.4, 0.03
lPEDSR	0.8 ± 0.16	0.8 ± 0.08	9.1	−0.03 ± 0.15	−0.3, 0.26
Haemodialysis patients (3-Tesla) (n = 10)					
GCS	−17.7 ± 2.9	−17.7 ± 2.6	5.4	0.01 ± 2	−3.9, 3.9
GLS	−14.4 ± 2.4	−14.4 ± 2.9	7	−0.02 ± 2.1	−4.2. 4.1
cPEDSR	0.96 ± 0.29	0.88 ± 0.25	11	0.08 ± 0.2	−0.3, 0.46
lPEDSR	0.8 ± 0.23	0.8 ± 0.18	11.4	0.0003 ± 0.2	−0.38, 0.38
All participants (both field strengths) (n = 30)					
GCS	−18.1 ± 3.1	−18.9 ± 2.5	6.6	0.9 ± 2.3	−3.6, 5.4
GLS	−15.3 ± 3.1	−15.5 ± 2.2	7.5	0.2 ± 2.3	−4.4, 4.8
cPEDSR	0.91 ± 0.2	0.94 ± 0.19	9.8	−0.03 ± 0.2	−0.39, 0.32
lPEDSR	0.77 ± 0.18	0.81 ± 0.15	11.5	−0.04 ± 0.18	−0.39, 0.32

CoV, co-efficent of variation; SD, standard deviation; BA, Bland-Altman; GCS, global circumferential strain; GLS, global longitudinal strain; cPEDSR, circumferential peak early diastolic strain rate; lPEDSR, longitudinal peak early diastolic strain rate.

reproducibility of FT-derived longitudinal PEDSR was significantly worse than TT-derived longitudinal PEDSR (p = 0.01). For patients with aortic stenosis and patients on haemodialysis, reproducibility of FT-derived longitudinal PEDSR was poorer than TT-derived longitudinal PEDSR, but this did not reach statistical significance (p = 0.36 and p = 0.29 respectively).

Bland-Altmann analysis did not reveal any systematic bias for any measures. There were tighter limits of agreement for TT-derived strain measures than FT-derived strain measures, with most data points within 95% confidence intervals for all measures (Fig. 3).

6. Interobserver variability of strain variables

Interobserver variability was excellent for all FT and TT derived strain measures (Table 3).

7. Sample size calculations

With the exception of GCS and circumferential PEDSR for haemodialysis patients and GCS for patients with diabetes, the sample sizes required to detect a 10% difference between study groups were smaller for TT than for FT for different strain parameters and patient groups (Table 4).

8. Discussion

The reproducibility of novel imaging techniques and software packages are routinely assessed in healthy volunteers but rarely in patient populations. We have compared the test-retest reproducibility of two commercially available software packages that derive strain measurements from SSFP cine images across a range of patient populations. Our findings highlight the importance of using the appropriate standard deviation and CoV of the patient population being investigated when calculating sample size requirements to avoid under or overestimation of the required sample size [24].

We have shown that the reproducibility of TT-derived peak systolic strain measures (GCS and GLS) are at least equivalent to the reproducibility of FT-derived peak systolic strain measures across a spectrum of disease states. We have also shown that the reproducibility of TT-derived circumferential PEDSR and longitudinal PEDSR are superior to

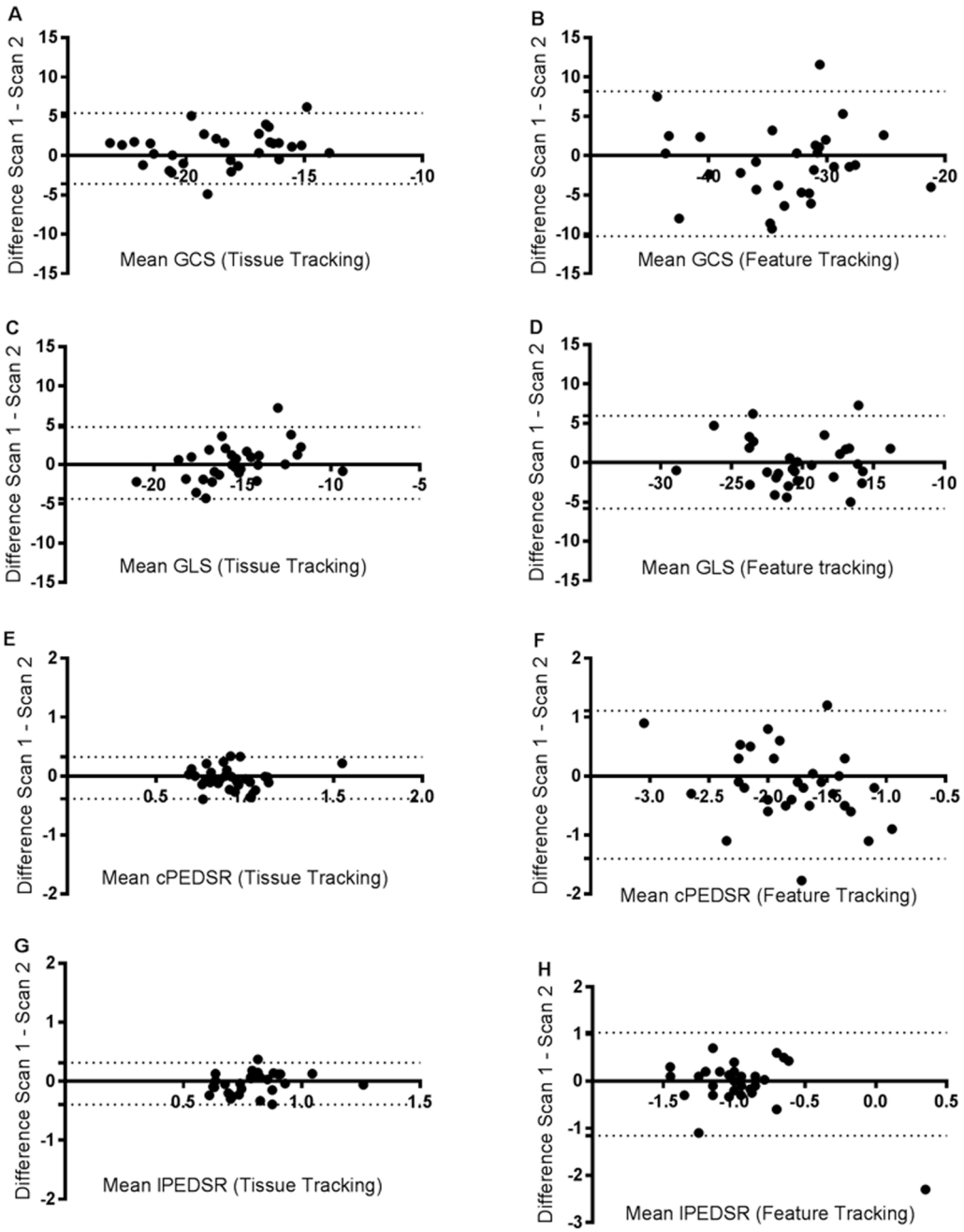

Fig. 3. Bland-Altman analysis of test-retest reproducibility of tissue tracking-derived and feature tracking derived strain parameters. GCS, global circumferential strain; GLS, global longitudinal strain; cPEDSR, circumferential peak early diastolic strain rate; lPEDSR, longitudinal peak early diastolic strain rate.

the reproducibility of FT-derived circumferential PEDSR and longitudinal PEDSR. These data alone have important implications when considering the software analysis for research studies and clinical workflow. The time taken to analyse strain with TT was significantly quicker than FT, however this was largely due to the time taken to load the contours into the FT software program. The TT software package used contours already created from LV volumetric analyses, avoiding duplication of contour drawing, streamlining workload. Cine-derived strain parameters are often not routinely included in clinical reports due to time constraints in analysis, and the requirements for additional, offline, software. The integration of TT into a comprehensive software analysis packages goes some way to rectifying these problems and for the first time one can see how reporting of strain may become a routine part of clinical reporting. As machine learning algorithms improve and automated quantification of LV volumes become more refined and used in clinical practice, the value of comprehensive software packages that include the ability to automatically calculate strain parameters will also increase.

In this study we were not primarily interested in the absolute strain values assess by FT and TT. As expeceted the strain values derived from FT software were globally higher than the absolute values derived from TT. This is quorate with previous studies that have shown the absolute strain values derived from FT analysis tend to be higher than those derived from tagged images [11]. With increasing evidence that FT-

Table 3
Interobserver variability of strain measiures assessed by feature tracking and tissue tracking.

	Observer 1	Observer 2	CoV (%)	Bias ± SD Difference	BA limits of agreement
Feature Tracking derived stain parameters					
Haemodialysis patients (3-Tesla) (n = 10)					
GCS	−30.6 ± 4.8	−32.6 ± 4.8	6.0	2.02 ± 3.4	−4.7, 8.7
GLS	−20.6 ± 2.7	−20.8 ± 3.4	4.2	0.18 ± 1.8	−3.4, 3.8
cPEDSR	1.8 ± 0.4	1.7 ± 0.4	5.3	−0.1 ± 0.2	−0.4, 0.3
lPEDSR	1.1 ± 0.1	1.0 ± 0.2	6.5	−0.07 ± 0.1	−0.3, 0.2
Tissue Tracking derived stain parameters					
Haemodialysis patients (3-Tesla) (n = 10)					
GCS	−18.6 ± 3.2	−18.3 ± 3.1	3.1	−0.2 ± 1.2	−2.5, 2.1
GLS	−14.4 ± 2.9	−15.0 ± 2.2	5.0	0.6 ± 1.4	−2.2, 3.4
cPEDSR	1.0 ± 0.3	1.0 ± 0.3	3.0	0.02 ± 0.06	−0.1, 0.1
lPEDSR	0.9 ± 0.3	0.9 ± 0.3	5.6	−0.01 ± 0.1	−0.2, 0.2

derived strain values are of independent, prognostic benefit in certain disease states [25], demonstrating the accuracy and reproducibility of these measurements becomes more important than the absolute agreement with strain derived from tagged images or other techniques, providing normal ranges for each technique and software can be established. To that end, strain values are known to vary depending on vendor software [26], such that absolute values cannot be directly used in clinical evaluation if different vendor software or analysis techniques are employed. In this study strain values are derived from the same short and long-axis cine images, so the differences between absolute numbers are largely to do with the differences in the software algorithms and the way they were employed. Similarly, because reproducibility was assessed on the same scans, the differences seen in reproducibility are largely related to the reproducibility of the software as the interobserver variability of both FT and TT was excellent for all strain parameters. Furthermore, the intraobserver variability of FT and TT derived strain have been shown to both be outstanding, even when undertaken on scans of patients with significant medical morbidity [11].

Our results suggest that the reproducibility of TT and FT-derived GCS and GLS are acceptable for use in clinical trials and longitudinal studies. However, for assessment of diastolic strain rates, our data indicate TT performed better in all patient groups at 3 T as well as 1.5 T. This study may suggest a need for standardization of cine-derived strain assessment, across CMR platforms and vendor software packages, including the establishment of normal ranges for different techniques and different vendor software packages at different field strengths (1.5-Tesla and 3-Tesla). Significant effort has been made in establishing normal values for different vendor software for strain derived from echocardiographic studies [27]. Indeed assessment of GLS with echocardiography is now a recommended part of multi-modality imaging evaluation of adult patients during and after cancer therapy [28]. Conducting similar work with CMR, may pave the way for strain assessment with CMR to be similarly, routinely adopted into clinical practice.

8.1. Limitations

This study has several limitations. We have not compared strain derived from cine images to strain derived from tissue tagging. This would have been important had we been evaluating the agreement between TT, FT and tissue tagging as has recently been done [11], but as the principle aim of this study was to assess the test-retest reproducibility cine derived strain measurements across disease states, tissue tagging was not included. We have included patients scanned at two field strengths. As each strain quantification technique was assessed in the same patients in the same field strength this is actually a strength of the study rather than a limitation. The time interval between scans varied between 4 and 11 days for each patient. We deliberately did not scan patients on the same day to allow more physiological variation between studies as this is more representative to what would happen in clinical practice or indeed in clinical research studies.

9. Conclusions

CMR-derived quantification of GCS and GLS is highly reproducible with both FT and TT software across a range of disease states. TT had excellent test-retest reproducibility for quantification of both longitudinal and circumferential PEDSR and was superior to FT-derived PEDSR. The discrete standard deviations and CoV of different disease populations must be determined to allow clinical trials to be appropriately powered.

Funding sources

This study is independent research arising from a Clinician Scientist Award (Dr James Burton, CS-2013-13-014) supported by the NIHR, an NIHR Career Development Fellowship (Gerald McCann NIHR-CDF 2014-07-045), and an NIHR grant (number PDF 2011-04-51 Gerald P McCann). This work is supported by the NIHR Leicester Cardiovascular Biomedical Research Unit based at University Hospitals of Leicester.

Table 4
Sample size needed to detect a 10% difference between two independent study groups with 80% and 90% power (alpha of 0.05) for each disease based on the mean and standard deviation of all interstudy scans. Studies of patients with aortic stenosis and patients on haemodialysis are calculated based on measures acquired at 3-Tesla, whilst studies of patient with diabetes are calculated based on measurements at 1.5-Tesla.

	Feature Tracking			Tissue Tracking		
	Mean ± SD	Sample Size (80% power)	Sample Size (90% power)	Mean ± SD	Sample Size (80% power)	Sample Size (90% power)
GCS HD patients	−31.5 ± 5.7	102	138	−17.7 ± 2.7	74	90
GLS HD patients	−19.3 ± 3.1	80	108	−14.4 ± 2.6	102	128
cPEDSR HD patients	1.76 ± 0.62	390	538	0.92 ± 0.27	270	350
lPEDSR HD patients	1.07 ± 0.26	186	234	0.80 ± 0.20	196	262
GCS patients with AS	−32.0 ± 5.1	90	122	−19.1 ± 2.3	46	60
GLS patients with AS	−18.5 ± 3.2	94	126	−15.5 ± 2.2	64	78
cPEDSR patients with AS	1.77 ± 0.47	222	296	0.91 ± 0.15	86	52
lPEDSR patients with AS	0.87 ± 0.28	326	436	0.79 ± 0.17	146	194
GCS patients with diabetes	−37.3 ± 5.7	74	98	−18.7 ± 3.3	98	130
GLS patients with diabetes	−23.0 ± 3.5	96	128	−16.3 ± 2.7	86	116
cPEDSR patients with diabetes	1.89 ± 0.61	328	420	0.94 ± 0.16	90	122
lPEDSR patients with diabetes	1.13 ± 0.28	192	272	0.79 ± 0.12	72	100

HD, haemodialysis; AS, aortic stenosis; GCS, global circumferential strain; GLS, global longitudinal strain; cPEDSR, circumferential peak early diastolic strain rate; lPEDSR, longitudinal peak early diastolic strain rate.

The views expressed in this publication are those of the authors and not necessarily those of the National Health Service, the National Institute for Health Research or the Department of Health.

Conflicts of interest

None of the authors have any relevant conflicts of interest to declare.

Acknowledgements

NA.

Appendix A. Supplementary data

Supplementary material related to this article can be found, in the online version, at doi:https://doi.org/10.1016/j.ejrad.2019.01.026.

References

[1] A.M. Shah, S.D. Solomon, Myocardial deformation imaging: current status and future directions, Circulation 17;125 (January (2)) (2012) 244.
[2] K. Kalam, P. Otahal, T.H. Marwick, Prognostic implications of global LV dysfunction: a systematic review and meta-analysis of global longitudinal strain and ejection fraction, Heart 100 (November (21)) (2014) 1673–1680.
[3] A.C. Ng, V. Delgado, M. Bertini, M.L. Antoni, R.J. van Bommel, E.P. van Rijnsoever, et al., Alterations in multidirectional myocardial functions in patients with aortic stenosis and preserved ejection fraction: a two-dimensional speckle tracking analysis, Eur Heart J. 32 (12) (2011) 1542–1550.
[4] D.A. Morris, L.H. Boldt, H. Eichstadt, C. Ozcelik, W. Haverkamp, Myocardial systolic and diastolic performance derived by 2-dimensional speckle tracking echocardiography in heart failure with normal left ventricular ejection fraction, Circ. Heart Fail. 1;5 (September (5)) (2012) 610–620.
[5] M.L. Antoni, S.A. Mollema, V. Delgado, J.Z. Atary, C.J. Borleffs, E. Boersma, et al., Prognostic importance of strain and strain rate after acute myocardial infarction, Eur. Heart J. 31 (July (13)) (2010) 1640–1647.
[6] E.H. Ibrahim, Myocardial tagging by cardiovascular magnetic resonance: evolution of techniques–pulse sequences, analysis algorithms, and applications, J. Cardiovasc. Magn. Reson. 13 (1) (2011) 36.
[7] M. Markl, S.B. Reeder, F.P. Chan, M.T. Alley, R.J. Herfkens, N.J. Pelc, Steady-state free precession MR imaging: improved myocardial tag persistence and signal-to-noise ratio for analysis of myocardial motion, Radiology 230 (3) (2004) 852–861.
[8] D.M. Harrild, Y. Han, T. Geva, J. Zhou, E. Marcus, A.J. Powell, Comparison of cardiac MRI tissue tracking and myocardial tagging for assessment of regional ventricular strain, Int. J. Cardiovasc. Imag. 28 (8) (2012) 2009–2018.
[9] K.N. Hor, R. Baumann, G. Pedrizzetti, G. Tonti, W.M. Gottliebson, M. Taylor, et al., Magnetic resonance derived myocardial strain assessment using feature tracking, J. Visual. Exp. (48) (2011).
[10] A. Padiyath, P. Gribben, J.R. Abraham, L. Li, S. Rangamani, A. Schuster, et al., Echocardiography and cardiac magnetic resonance-based feature tracking in the assessment of myocardial mechanics in tetralogy of fallot: an intermodality comparison, Echocardiography 30 (2) (2013) 203–210.
[11] J.J. Cao, N. Ngai, L. Duncanson, J. Cheng, K. Gliganic, Q. Chen, A comparison of both DENSE and feature tracking techniques with tagging for the cardiovascular magnetic resonance assessment of myocardial strain, J. Cardiovasc. Magn. Reson. 20 (1) (2018) 26.
[12] A. Singh, J.P. Greenwood, C. Berry, D.K. Dawson, K. Hogrefe, D.J. Kelly, et al., Comparison of exercise testing and CMR measured myocardial perfusion reserve for predicting outcome in asymptomatic aortic stenosis: the PRognostic importance of MIcrovascular dysfunction in aortic stenosis (PRIMID AS) study, Eur. Heart J. (2017).
[13] M.P.M. Graham-Brown, D.S. March, D.R. Churchward, H.M.L. Young, M. Dungey, S. Lloyd, et al., Design and methods of CYCLE-HD: improving cardiovascular health in patients with end stage renal disease using a structured programme of exercise: a randomised control trial, BMC Nephrol. 17 (1) (2016) 69.
[14] A. Singh, I. Ford, J.P. Greenwood, J.N. Khan, A. Uddin, C. Berry, et al., Rationale and design of the PRognostic importance of MIcrovascular dysfunction in asymptomatic patients with aortic stenosis (PRIMID-AS): a multicentre observational study with blinded investigations, BMJ Open. 18;3 (December (12)) (2013) 004348.
[15] C.D. Steadman, M. Jerosch-Herold, B. Grundy, S. Rafelt, L.L. Ng, I.B. Squire, et al., Determinants and functional significance of myocardial perfusion reserve in severe aortic stenosis, Cardiovasc. Imag. 5 (2) (2012) 182–189.
[16] A. Singh, C.D. Steadman, J.N. Khan, M.A. Horsfield, S. Bekele, S.A. Nazir, et al., Intertechnique agreement and interstudy reproducibility of strain and diastolic strain rate at 1.5 and 3 tesla: A comparison of feature-tracking and tagging in patients with aortic stenosis, J. Magn. Reson. Imaging 41 (4) (2015) 1129–1137.
[17] M.P. Graham-Brown, D.S. March, D.R. Churchward, D.J. Stensel, A. Singh, R. Arnold, et al., Novel cardiac nuclear magnetic resonance method for noninvasive assessment of myocardial fibrosis in hemodialysis patients, Kidney Int. 90 (4) (2016) 835–844.
[18] M.P. Graham-Brown, E. Rutherford, E. Levelt, D.S. March, D.R. Churchward, D.J. Stensel, et al., Native T1 mapping: inter-study, inter-observer and inter-center reproducibility in hemodialysis patients, J Cardiovasc. Magn. Reson. 19 (1) (2017) 21.
[19] K.N. Hor, W.M. Gottliebson, C. Carson, E. Wash, J. Cnota, R. Fleck, et al., Comparison of magnetic resonance feature tracking for strain calculation with harmonic phase imaging analysis, Cardiovasc. Imag. 3 (2) (2010) 144–151.
[20] J.M. Bland, D. Altman, Statistical methods for assessing agreement between two methods of clinical measurement, Lancet 327 (8476) (1986) 307–310.
[21] M. Bland, An Introduction to Medical Statistics, Oxford University Press, UK), 2015.
[22] F. Grothues, G.C. Smith, J.C. Moon, N.G. Bellenger, P. Collins, H.U. Klein, et al., Comparison of interstudy reproducibility of cardiovascular magnetic resonance with two-dimensional echocardiography in normal subjects and in patients with heart failure or left ventricular hypertrophy, Am. J. Cardiol. 1;90 (July (1)) (2002) 29–34.
[23] B. Rosner, Fundamentals of Biostatistics, Brooks/Cole, Boston, 2011.
[24] G. Morton, A. Schuster, R. Jogiya, S. Kutty, P. Beerbaum, E. Nagel, Inter-study reproducibility of cardiovascular magnetic resonance myocardial feature tracking, J. Cardiovasc. Magn. Reson. 14 (1) (2012) 43.
[25] M. Chimura, T. Onishi, Y. Tsukishiro, T. Sawada, K. Kiuchi, A. Shimane, et al., Longitudinal strain combined with delayed-enhancement magnetic resonance improves risk stratification in patients with dilated cardiomyopathy, Heart (2016) 309746.
[26] A. Schuster, V. Stahnke, C. Unterberg-Buchwald, J.T. Kowallick, P. Lamata, M. Steinmetz, et al., Cardiovascular magnetic resonance feature-tracking assessment of myocardial mechanics: intervendor agreement and considerations regarding reproducibility, Clin. Radiol. 70 (9) (2015) 989–998.
[27] R.M. Lang, L.P. Badano, V. Mor-Avi, J. Afilalo, A. Armstrong, L. Ernande, et al., Recommendations for cardiac chamber quantification by echocardiography in adults: an update from the American society of echocardiography and the European association of cardiovascular imaging, J. Am. Soc. Echocardiogr. 28 (1) (2015) 39 e14.
[28] J.C. Plana, M. Galderisi, A. Barac, M.S. Ewer, B. Ky, M. Scherrer-Crosbie, et al., Expert consensus for multimodality imaging evaluation of adult patients during and after cancer therapy: a report from the American society of echocardiography and the European association of cardiovascular imaging, J. Am. Soc. Echocardiogr. 27 (9) (2014) 911–939.